AAS 05-161

MODELING AND CONTROL OF INTERFEROMETRIC FORMATIONS IN THE VICINITY OF THE COLLINEAR LIBRATION POINTS

Prasenjit Sengupta* **and Srinivas R. Vadali†**

The modeling and control of a Fizeau-type interferometer in the elliptic, restricted three-body problem of the Sun and Earth-Moon Barycenter system, is the subject of this paper. The interferometer is in a quasi-periodic (Lissajous) orbit about the trans-terrestrial libration point. Control laws are derived for effective station-keeping, inertial and local pointing, and slewing maneuvers, as well as attitude maintenance of the spacecraft in the formation. These control laws are derived from candidate Lyapunov functions, each of which is proven to be globally and asymptotically stable. The approach in this paper couples the translational and attitude kinematics of the spacecraft, thereby leading to a more accurate representation of the system. Simulations are provided for various types of maneuvers.

INTRODUCTION

The Circular Restricted Three-Body Problem (CR3BP), is a special case of the Elliptic Restricted Three-Body Problem (ER3BP), both of which have historically been topics of great interest. This is due to the fact that both are important steps to the design analysis of many real-world astrodynamical problems of today, such as interplanetary trajectories and deep-space missions. The CR3BP studies the motion of a small mass, such as a spacecraft in a system comprising two massive primaries, such as the Earth and Moon, or the Sun and Jupiter, that mutually revolve in circular orbits about their center of mass. The ER3BP includes eccentricity effects of the primaries' motion, by assuming that the smaller primary rotates about the larger primary in two-body Keplerian motion. While the CR3BP has one integral of motion, the time-varying nature of the Hamiltonian of the ER3BP renders this missing in the latter case, and many phenomena such as the surfaces of zero velocity, etc. are no longer observed. However, the ER3BP more closely resembles physical realities, since eccentricities in the planetary system are of levels that cannot be neglected.

*Graduate Student, Department of Aerospace Engineering, Texas A&M University, College Station, TX 77843-3141, prasenjit@tamu.edu, Student Member, AAS.

†Stewart & Stevenson-I Professor, Department of Aerospace Engineering, Texas A&M University, College Station, TX 77843-3141, svadali@aero.tamu.edu.

The CR3BP/ER3BP admit five equilibrium points in the rotating frame, known as Lagrangian/Libration points. Of these, three lie on the line passing through the primaries. These points, denoted by L_3 (on the outside of the larger primary), L_1 (between the primaries), and L_2 (on the outside of the smaller primary), have been viewed with great interest since the latter half of the last century. For the Sun-Earth-Moon (SEM) system, the points L_1 and L_2 are of greater interest than L_3 due to the latter's proximity to the Sun. Though these equilibria are unstable, the system allows for the existense of periodic (halo) and quasi-periodic (Lissajous) trajectories about them. These orbits are also unstable; however they prove useful in the form of reference trajectories for formations. Various missions have been proposed to successfully utilize halo/Lissajous orbits, such as the ISEE-3/ICE, SI, and TPF[1–3] among others. A thorough survey of the dynamics associated with these points is presented in Ref. 4.

There exist many approaches to obtain periodic and quasi-periodic trajectories about the libration points. Perturbation techniques have been used with great efficacy on systems where the gravitational potential has been expanded to second-, third- and fourth-order terms using Legendre polynomials.[5–7] These methods provide analytical expressions for trajectories that account for eccentricity and lunar/solar perturbations, and provide an excellent starting point for the generation of numerically accurate trajectories. An algorithm developed by Howell and Pernicka[8] is used in a modified manner, that takes into account the time-variant nature of the ER3BP, to generate a Lissajous trajectory of required dimensions about the L_2 point of the SEM system.

Stationkeeping of a satellite in a libration point trajectory depends on an accurate representation of the nominal trajectory. Effective algorithms have been developed that reduce the burden of storage of points generated via the numerical approach, and instead use the state transition matrix for correction calculations.[9] The algorithm in this reference uses impulsive thrusts at different intervals for orbit correction. In this paper, for the sake of simplicity, quintic interpolation is used to generate nominal trajectories. Continuous control is used to stabilize the satellite about this trajectory.

The interferometer is modeled as a formation of rigid satellites about the libration point. This results in the study of both the translational equation of motion as well as attitude kinematics, and coupling effects need to be studied. A useful survey of existing methodologies for stationkeeping control of formations is presented in Ref. 10. Stationkeeping methodologies have also been developed for formations in halo orbits about the L_2 point of the SEM system, in Ref. 11. Folta[12] analyzes the problem of interferometric satellite stationkeeping in the vicinity of libration points, under a variety of maneuvers. Ren and Beard[13] derive feedback control laws for the motion of virtual structures in space.

This paper begins by addressing the problem of attitude kinematics as well as translational motion by first considering a rigid satellite in the ER3BP, with position-attitude coupling, introduced by the gravity-gradient torque. Reference 14 analyzes the attitude kinematics of a rigid satellite, but is limited to the planar case and single-axis rotation. In this case, however, an interferometric formation in a large Lissajous orbit requires a more generalized approach. Next, a Lissajous trajectory is determined numerically, followed by the modeling of the distributed Fizeau interferometer. Control laws from a Lyapunov ap-

proach[15] are developed for a variety of maneuvers and for station-keeping, as well as attitude control, that account for gravity-gradient torque as well as torques arising due to solar radiation pressure (SRP), which affect the system to a greater degree than the gravity-gradient torque. The advantage of formation rotation is demonstrated for different types of maneuvers. Numerical examples are used to demonstrate the the dynamics and control of the interferometer.

TRANSLATION AND ATTITUDE KINEMATICS OF A SATELLITE IN THE ELLIPTIC RESTRICTED THREE-BODY PROBLEM

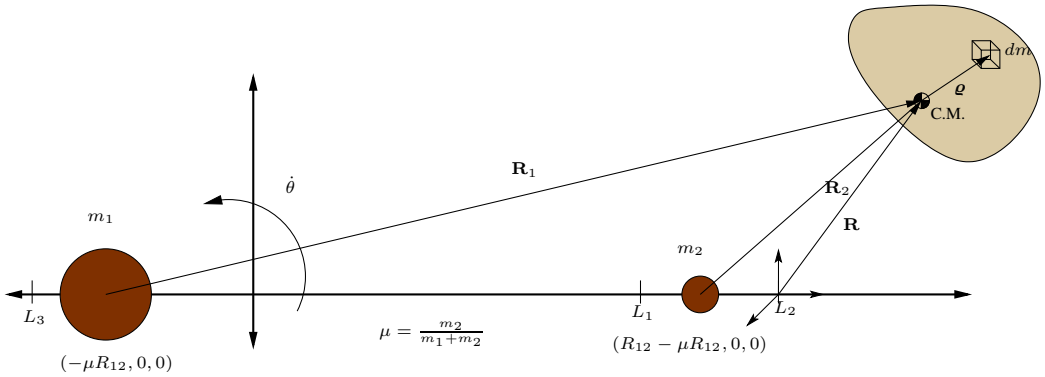

Figure 1. Rigid Satellite in the Elliptic Restricted Three-Body Problem

Consider the elliptic restricted three body problem, with a rotating frame at the center of mass of the two primaries. This frame, denoted by $\mathcal{E}$, has as basis vectors, $\mathbf{e}_i$, $i = 1 \ldots 3$, and rotates with angular velocity $\dot{\theta}\mathbf{e}_3$, with respect to the inertial frame, $\mathcal{N}$. Also consider the body frame of the rigid body, denoted by $\mathcal{B}$, which coincides with the principal axes of the satellite, and has basis vectors $\mathbf{b}_i$, $i = 1 \ldots 3$. The vector $\mathbf{b}_1$ is assumed to be in the direction of the axis of the mirror array. Let the orientation of $\mathcal{B}$ with respect to $\mathcal{E}$ be given by the direction cosine matrix $\mathbf{C}$. The matrix $\mathbf{C}$ can be characterized by any suitable set of parameters, for e.g., Euler angles. The use of Euler parameters is preferred, due to the lack of singularities associated with an Euler angle description.

For the purpose of halo/Lissajous orbit analysis, the origin of the rotating frame is shifted to the Lagrangian point under consideration (in this case, L_2). The Lagrangian point is placed at a distance $\gamma_L R_{12}$ on the right of the second primary m_2, where R_{12} is the time-varying distance between the two primaries, given by $R_{12} = a(1 - e\cos E)$. The rate of rotation of the frame, $\dot{\theta}$ is not a constant, and is given by $\dot{\theta} = \sqrt{G(m_1 + m_2)a(1 - e^2)}/R_{12}^2$.

Translation Equations of Motion of the Satellite

The equations of motion for the translation of a rigid satellite are obtained directly from a Lagrangian formulation for the system by first obtaining the expressions for potential energy arising due to the gravitational fields of the two primaries, and the kinetic energy arises due to the translation as well as rotation[16] of the satellite. The equations of motion in ER3BP have been derived in Ref. 4. In this paper, rigid body effects are also added to the expression for potential energy. The following normalization is performed: 1) total

mass of the primaries is 1 (the mass of the smaller primary is thus μ), 2) length is scaled by semimajor axis a, and 3) time period of rotation is 2π. Furthermore, the inertia tensor of the satellite, denoted by $\mathcal{I}_K$ (in the $\mathcal{K}$ frame), is normalized with the quantity ma^2, where m is the mass of the spacecraft, to yield $\mathbf{I}_K$. Without loss of generality, the inertia tensor in the body frame, $\mathbf{I}_B$, is denoted by $\mathbf{I}$. Let $\mathbf{r}_i$ denote the normalized position vector of the satellite center of mass with respect to each primary, and let $\mathscr{R}_i = \mathbf{C}\mathbf{r}_i$ denote the transformation of this vector into the body frame. It can thus be shown that the normalized potential energy is given by:

$$\begin{aligned}\mathcal{V} &= -\frac{1}{ma^2n^2}\left[\int_B \frac{Gm_1}{|\mathbf{R}_1+\boldsymbol{\varrho}|}\,dm + \int_B \frac{Gm_2}{|\mathbf{R}_2+\boldsymbol{\varrho}|}\,dm\right] \\ &= -\left(\frac{1-\mu}{r_1}+\frac{\mu}{r_2}\right) - \frac{1}{2}\left(\frac{1-\mu}{r_1^3}+\frac{\mu}{r_2^3}\right)\mathrm{tr}\mathbf{I} + \frac{3}{2}\left(\frac{1-\mu}{r_1^5}\mathscr{R}_1{}^T\mathbf{I}\mathscr{R}_1 + \frac{\mu}{r_2^5}\mathscr{R}_2{}^T\mathbf{I}\mathscr{R}_2\right) \quad (1)\end{aligned}$$

It is also shown in Ref. 4 that the velocity of the satellite mass center is of the following form:

$$\begin{aligned}\dot{\mathbf{r}} = &\quad [\dot{x}+(1-\mu+\gamma_L)\dot{\rho}-(1+\nu)y]\,\mathbf{e}_1 \\ &+ [\dot{y}+(1+\nu)x+(1+\nu)(1-\mu+\gamma_L)(1+\rho)]\,\mathbf{e}_2 \\ &+ \dot{z}\mathbf{e}_3\end{aligned} \quad (2)$$

where, the quantities ρ and ν correspond to the normalized two-body distance and true anomaly arising from the Keplerian rotation of the Earth-Moon barycenter about the Sun:

$$1+\nu = \frac{\dot{\theta}}{n} = \frac{\left(1-e^2\right)^{\frac{1}{2}}}{\left(1-e\cos E\right)^2} \quad (3)$$

$$1+\rho = \frac{R}{a} = 1-e\cos E \quad (4)$$

The normalized translational kinetic energy is given by the expression $\mathcal{T}_{\mathrm{trans}} = \frac{1}{2}\dot{\mathbf{r}}\cdot\dot{\mathbf{r}}$.

Let the inertial angular velocity of the frame $\mathcal{B}$ be $\boldsymbol{\omega} = \omega_1\mathbf{b}_1 + \omega_2\mathbf{b}_2 + \omega_3\mathbf{b}_3$. Since $\mathcal{B}$ coincides with the principal axes of the the rigid body, this is also the angular velocity of the body expressed in its own frame. Furthermore, the inertia tensor $\mathbf{I}$ in this frame, is diagonal. Let the diagonal elements of this inertial tensor be I_i, $i = 1\ldots3$. The rotational kinetic energy is thus given by $\mathcal{T}_{\mathrm{rot}} = \frac{1}{2}\boldsymbol{\omega}\cdot(\mathbf{I}_B\boldsymbol{\omega})$.

From the expressions for potential and kinetic energy, the Lagrangian of the system is $\mathcal{L} = \mathcal{T}_{\mathrm{trans}} + \mathcal{T}_{\mathrm{rot}} - \mathcal{V}$. The translational equations of motion are thus:

$$\begin{aligned}&\ddot{x} - 2(1+\nu)\dot{y} + (1+\gamma_L)\ddot{\rho} - \dot{\nu}y - (1+\nu)^2\left[(1+\gamma_L)(1+\rho)+x\right] = \\ &-\frac{(1-\mu)}{r_1^3}\left[(1+\gamma_L)(1+\rho)+x\right]\left(1+\frac{3}{2}\frac{\mathrm{tr}\mathbf{I}}{r_1^2} - \frac{15}{2}\frac{\mathscr{R}_1{}^T\mathbf{I}\mathscr{R}_1}{r_1^4}\right) - 3\frac{(1-\mu)}{r_1^5}\mathbf{c}_1^T\mathbf{I}\mathscr{R}_1 \\ &-\frac{\mu}{r_2^3}\left[\gamma_L(1+\rho)+x\right]\left(1+\frac{3}{2}\frac{\mathrm{tr}\mathbf{I}}{r_2^2} - \frac{15}{2}\frac{\mathscr{R}_2{}^T\mathbf{I}\mathscr{R}_2}{r_2^4}\right) - 3\frac{\mu}{r_2^5}\mathbf{c}_1^T\mathbf{I}\mathscr{R}_2 - \frac{\mu}{(1+\rho)^2} \quad (5a) \\ &\ddot{y} + 2(1+\nu)\left[(1+\gamma_L)\dot{\rho}+\dot{x}\right] + \dot{\nu}\left[(1+\gamma_L)(1+\rho)+x\right] - (1+\nu)^2 y =\end{aligned}$$

$$
\begin{aligned}
&-\frac{(1-\mu)y}{r_1^3}\left(1+\frac{3}{2}\frac{\mathrm{tr}\mathbf{I}}{r_1^2}-\frac{15}{2}\frac{{\mathscr{R}_1}^T\mathbf{I}\mathscr{R}_1}{r_1^4}\right)-3\frac{(1-\mu)}{r_1^5}\mathbf{c}_2^T\mathbf{I}\mathscr{R}_1\\
&-\frac{\mu y}{r_2^3}\left(1+\frac{3}{2}\frac{\mathrm{tr}\mathbf{I}}{r_2^2}-\frac{15}{2}\frac{{\mathscr{R}_2}^T\mathbf{I}\mathscr{R}_2}{r_2^4}\right)-3\frac{\mu}{r_2^5}\mathbf{c}_2^T\mathbf{I}\mathscr{R}_2 \qquad (5b)\\
\ddot{z}=&-\frac{(1-\mu)z}{r_1^3}\left(1+\frac{3}{2}\frac{\mathrm{tr}\mathbf{I}}{r_1^2}-\frac{15}{2}\frac{{\mathscr{R}_1}^T\mathbf{I}\mathscr{R}_1}{r_1^4}\right)-3\frac{(1-\mu)}{r_1^5}\mathbf{c}_3^T\mathbf{I}\mathscr{R}_1\\
&-\frac{\mu z}{r_2^3}\left(1+\frac{3}{2}\frac{\mathrm{tr}\mathbf{I}}{r_2^2}-\frac{15}{2}\frac{{\mathscr{R}_2}^T\mathbf{I}\mathscr{R}_2}{r_2^4}\right)-3\frac{\mu}{r_2^5}\mathbf{c}_3^T\mathbf{I}\mathscr{R}_2 \qquad (5c)
\end{aligned}
$$

where, $\mathbf{c}_i$ is the ith column of the matrix $\mathbf{C}$.

Of interest is the weak coupling between attitude and translation introduced by the normalized inertia tensor $\mathbf{I}$. To estimate the relative magnitude of this inertial coupling, assume the satellite is modeled as a disc of radius R. Then the contribution of rigid body effects is $\mathcal{O}(R^2/a^2)$. In the Sun-Earth system, $a \approx 1.5\times10^8$km, and $\gamma_L \approx 0.01$. Even if the satellite has radius 0.15km, and is placed near L_2, then $r_1=\mathcal{O}(1)$ and $r_2=\mathcal{O}(\gamma_L)$. The relative contribution of the inertial terms in Eq. (5) is approximately 1×10^{-18}. To compare with eccentricity effects, consider the estimate: $(1+\gamma_L)\ddot{\rho}=\mathcal{O}(e)$. For the Sun-Earth system, $e=0.016$. Thus, for the present analysis, the terms involving moments of inertia may be dropped, and Eq. (5) reduce to the form:[4]

$$
\begin{aligned}
\ddot{\mathbf{x}} &= \mathbf{f}(\mathbf{x},\dot{\mathbf{x}})=\{f_1(\mathbf{x},\dot{\mathbf{x}}) \quad f_2(\mathbf{x},\dot{\mathbf{x}}) \quad f_3(\mathbf{x},\dot{\mathbf{x}})\}^T \qquad (6)\\
f_1(\mathbf{x},\dot{\mathbf{x}}) &= 2(1+\nu)\dot{y}-(1+\gamma_L)\ddot{\rho}+\dot{\nu}y+(1+\nu)^2\left[(1+\gamma_L)(1+\rho)+x\right]\\
&\quad -\frac{(1-\mu)}{r_1^3}\left[(1+\gamma_L)(1+\rho)+x\right]-\frac{\mu}{r_2^3}\left[\gamma_L(1+\rho)+x\right]-\frac{\mu}{(1+\rho)^2}\\
f_2(\mathbf{x},\dot{\mathbf{x}}) &= -2(1+\nu)\left[(1+\gamma_L)\dot{\rho}+\dot{x}\right]-\dot{\nu}\left[(1+\gamma_L)(1+\rho)+x\right]+(1+\nu)^2y\\
&\quad -\frac{(1-\mu)y}{r_1^3}-\frac{\mu y}{r_2^3}\\
f_3(\mathbf{x},\dot{\mathbf{x}}) &= -\frac{(1-\mu)z}{r_1^3}-\frac{\mu z}{r_2^3}
\end{aligned}
$$

Attitude Kinematics of the Satellite

Though the attitude of the satellite has been shown have negligible effects on the translational motion, the converse is not necessarily true, and expresses itself through the gravity-gradient torque. The nondimensional gravity-gradient torque induced by both primaries can be shown to be of the following form:

$$
\boldsymbol{\tau}_g=\frac{1}{n^2\mathrm{tr}\mathcal{I}}\int_B \boldsymbol{\varrho}\times\ d\mathbf{f}_g=3\frac{(1-\mu)}{r_1^5}\widetilde{\mathbf{r}}_1\mathbf{I}_E\mathbf{r}_1+3\frac{\mu}{r_2^5}\widetilde{\mathbf{r}}_2\mathbf{I}_E\mathbf{r}_2 \qquad (7)
$$

where $\widetilde{\mathbf{r}}_i$ denotes the cross-product tensor associated with $\mathbf{r}_i$, and the inertia tensor is normalized with respect to its trace.

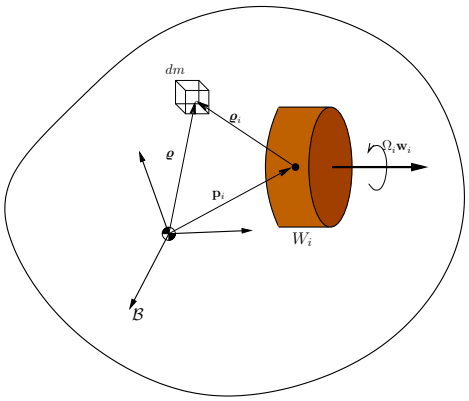

Figure 2. Rigid Satellite and the ith Momentum Wheel

To obtain the expression for force and torque arising due to SRP, it is assumed without loss of generality that the direction $\mathbf{b}_1$ corresponds to the normal vector of the SRP area. Thus, the SRP force is shown to have the following form:[17]

$$\mathbf{f}_{\text{SRP}} = -P_S A \left[2\rho_S \left(\mathbf{b}_1 \cdot \mathbf{s} \right)^2 \mathbf{b}_1 + \rho_A \left(\mathbf{b}_1 \cdot \mathbf{s} \right) \mathbf{s} + \rho_D \left(\mathbf{b}_1 \cdot \mathbf{s} \right) \left(\mathbf{s} + \frac{2}{3} \mathbf{b}_1 \right) \right] \tag{8}$$

In the above expression, P_S is the solar radiation pressure, which is assumed constant and equal to $P_S = 4.644 \times 10^{-6} \text{N/m}^2$. The surface area of the satellite affected by SRP is denoted by A. The coefficients ρ_S, ρ_A and ρ_D, denote respectively, the specular reflection, the absorption, the diffusion, and have their sum equal to 1. These quantities are determined by the physical characteristics of the satellite. The vector $\mathbf{s}$ denotes the direction of rays from the Sun. In the frame $\mathcal{E}$, this vector is a constant with $\mathbf{s} = -\mathbf{e}_1$. Consequently, to obtain this vector in frame $\mathcal{B}$, a transformation using the corresponding direction cosine matrix must be performed. The SRP results in a torque on the satellite, if the center of pressure does not coincide with the center of mass. If the position of the center of pressure with respect to the center of mass in $\mathcal{B}$ is denoted by $\mathbf{r}_{\text{cp}}$, then the SRP torque is evaluated as $\boldsymbol{\tau}_s = \mathbf{r}_{\text{cp}} \times \mathbf{f}_{\text{SRP}} / (n^2 \text{tr}\mathcal{I})$. Together, the gravity-gradient and SRP torques comprise the disturbance torque, denoted by $\boldsymbol{\tau}_d$.

An arbitrarily-shaped spacecraft with momentum wheels is considered.[18] Let the satellite have m momentum wheels, and consider the ith momentum wheel, denoted by W_i, whose center of mass is at $\mathbf{p}_i = p_{i_1} \mathbf{b}_1 + p_{i_2} \mathbf{b}_2 + p_{i_2} \mathbf{b}_3$ (dimensional quantity) with respect to the center of mass of the spacecraft. This wheel has axis of rotation in the direction $\mathbf{w}_i$ (in the $\mathcal{B}$ frame), and rotates with normalized angular velocity $\boldsymbol{\Omega}_i^B = \Omega_i \mathbf{w}_i$, relative to $\mathcal{B}$. If $\mathbf{Q}_i$ is the direction cosine matrix of the wheel-centered frame, denoted by $\mathcal{W}_i$, then $\mathbf{w}_i = Q_{i_{11}} \mathbf{b}_1 + Q_{i_{12}} \mathbf{b}_2 + Q_{i_{13}} \mathbf{b}_3$. The inertia tensor in $\mathcal{W}_i$, which is also the principal inertia tensor, is expressed as

$$\mathbf{J}_{W_i} = \begin{bmatrix} J_{i_a} & 0 & 0 \\ 0 & J_{i_t} & 0 \\ 0 & 0 & J_{i_t} \end{bmatrix}$$

where J_{i_a} is the moment of inertia in the axial direction and J_{i_t}, in the transverse directions (each normalized by $\text{tr}\mathcal{I}_B$). Let the relative wheel momenta be defined as $h_i = J_{i_a} \Omega_i$ and

the motor torque acting on the ith wheel, as u_i. It can be shown[18] that the modified Euler equations for the attitude kinematics of the the spacecraft take the following form:

$$\left(\overline{\mathbf{I}} - \overline{\mathbf{Q}}\mathbf{J}_a\overline{\mathbf{Q}}^T\right)\dot{\boldsymbol{\omega}} = -\widetilde{\boldsymbol{\omega}}\left(\overline{\mathbf{I}}\boldsymbol{\omega} + \overline{\mathbf{h}}\right) + \boldsymbol{\tau}_d - \overline{\mathbf{u}} \tag{9a}$$

$$\dot{\overline{\mathbf{h}}} = \overline{\mathbf{u}} - \overline{\mathbf{Q}}\mathbf{J}_a\overline{\mathbf{Q}}^T\dot{\boldsymbol{\omega}} \tag{9b}$$

where, $\overline{\mathbf{h}}$ and $\overline{\mathbf{u}}$ are the generalized wheel moment vector and generalized motor torque vector respectively, with $\overline{\mathbf{h}} = \overline{\mathbf{Q}}\mathbf{h}$ and $\overline{\mathbf{u}} = \overline{\mathbf{Q}}\mathbf{u}$. Furthermore,

$$\overline{\mathbf{I}} = \mathbf{I} + \sum_{i=1}^{m}\frac{m_i}{\mathrm{tr}\mathcal{I}_B}\begin{bmatrix} p_{i_2}^2 + p_{i_2}^2 & -p_{i_1}p_{i_2} & -p_{i_1}p_{i_2} \\ -p_{i_2}p_{i_1} & p_{i_2}^2 + p_{i_1}^2 & -p_{i_2}p_{i_2} \\ -p_{i_2}p_{i_1} & -p_{i_2}p_{i_2} & p_{i_1}^2 + p_{i_2}^2 \end{bmatrix} + \sum_{i=1}^{m}\mathbf{Q}_i^T\mathbf{J}_{W_i}\mathbf{Q}_i$$

$$\overline{\mathbf{Q}} = \begin{bmatrix}\overline{\mathbf{q}}_{1_1}^T & \overline{\mathbf{q}}_{2_1}^T & \cdots & \overline{\mathbf{q}}_{m_1}^T\end{bmatrix}$$

$$\mathbf{h} = \{h_1 \cdots h_m\}^T$$

$$\mathbf{u} = \{u_1 \cdots u_m\}^T$$

$$\mathbf{J}_a = \begin{bmatrix} J_{1_a} & \cdots & 0 \\ \vdots & \ddots & \vdots \\ 0 & \cdots & J_{m_a} \end{bmatrix}$$

and $\overline{\mathbf{q}}_{i_1}$ is the first row of $\mathbf{Q}_i$.

The attitude of the satellite is expressed through the use of Euler parameters (EPs). Let $\boldsymbol{\beta} = \{\beta_0 \quad \beta_1 \quad \beta_2 \quad \beta_3\}^T$ be the EPs characterizing the orientation of $\mathcal{B}$ with respect to $\mathcal{N}$. Then, the rate of change of $\boldsymbol{\beta}$ is related to the non-dimensionalized inertial angular velocity, $\boldsymbol{\omega}$, by the following:

$$\begin{aligned}\dot{\boldsymbol{\beta}} &= \frac{1}{2}\mathbf{B}(\boldsymbol{\beta})\begin{Bmatrix} 0 \\ \boldsymbol{\omega} \end{Bmatrix} \\ \mathbf{B}(\boldsymbol{\beta}) &= \begin{bmatrix} \beta_0 & -\beta_1 & -\beta_2 & -\beta_3 \\ \beta_1 & \beta_0 & -\beta_3 & \beta_2 \\ \beta_2 & \beta_3 & \beta_0 & -\beta_1 \\ \beta_3 & -\beta_2 & \beta_1 & \beta_0 \end{bmatrix}\end{aligned} \tag{11}$$

The EPs corresponding to the rotating frame can be shown to be:

$$\beta_{E_0} = \cos\frac{\theta}{2}, \quad \beta_{E_1} = \beta_{E_2} = 0, \quad \beta_{E_3} = \sin\frac{\theta}{2} \tag{12}$$

Thus, if $\boldsymbol{\beta}_{B/E}$ is the EP set characterizing the orientation of $\mathcal{B}$ with respect to $\mathcal{E}$ (i.e., orientation of the spacecraft in the rotating frame), then

$$\boldsymbol{\beta}_{B/E} = \begin{bmatrix} \beta_{B_0} & \beta_{B_1} & \beta_{B_2} & \beta_{B_3} \\ \beta_{B_1} & -\beta_{B_0} & -\beta_{B_3} & \beta_{B_2} \\ \beta_{B_2} & \beta_{B_3} & -\beta_{B_0} & -\beta_{B_1} \\ \beta_{B_3} & -\beta_{B_2} & \beta_{B_1} & -\beta_{B_0} \end{bmatrix}\boldsymbol{\beta}_E \tag{13}$$

GENERATING NOMINAL LISSAJOUS ORBITS

The Lissajous orbit that is used as a reference orbit is obtained numerically, by first using an analytical solution with the desired parameters, from Ref. 7, as initial guesses to obtain target points. A series of two-point boundary value problems using the shooting method are solved to first render the trajectory continuous in position, followed by velocity discrepancy reduction at the target points, as shown in Ref. 8. The second step requires forward and backward integration of the system of equations, and the state transition matrix of the ER3BP differs to some extent from that of the CR3BP. Thus the algorithm is modified slightly, in the propagation of the state transition matrix $\mathbf{\Phi}(t, t_0)$ using the Jacobian of the system, $\mathbf{F}$ that obtained through the linearization of Eq. (6):

$$\dot{\mathbf{\Phi}}(t, t_0) = \mathbf{F}(t)\mathbf{\Phi}(t, t_0) \tag{14}$$

$$\mathbf{F} = \begin{bmatrix} \mathbb{O}_{3\times3} & \mathbb{1}_{3\times3} \\ \mathbf{A} & \mathbf{\Omega} \end{bmatrix} \tag{15}$$

$$\mathbf{\Omega} = 2(1+\nu)\begin{bmatrix} 0 & 1 & 0 \\ -1 & 0 & 0 \\ 0 & 0 & 0 \end{bmatrix}$$

The matrix $\mathbf{A}$, has as its elements the derivatives of $\mathbf{f}(\mathbf{x})$ in Eq. (6), with respect to x, y, and z, respectively, and is not symmetric due to eccentricity effects.

Using the method outlined above, a Lissajous trajectory with y and z amplitudes approximately 300,000km is designed, using 40 segments for 6 years. The resulting Lissajous orbit is shown in Figure 3. This orbit is found to have an out-of-plane period of approximately 6 months.

INTERFEROMETER MODELING

The interferometer considered here is designed keeping one satellite on the Lissajous orbit with the purpose of collection and combining the data, and using several satellites placed in a formation in the neighborhood of the primary satellite, that act as receptors. The primary satellite that is on the Lissajous orbit will be referred to as the 'focal' satellite, and the other satellites will be referred to as the 'mirror' satellites.

The interferometer has associated with it, a line-of-site (LOS) vector, that points in the direction of interest. This direction may be fixed inertially, or rotate at a given rate, depending on the mission requirements. The focal and mirror satellites are placed relative to each other in a local frame, $\mathcal{D}$, with origin on the Lissajous orbit, and has basis vectors $\mathbf{d}_i$, $i = 1 \ldots 3$. The unit vector $\mathbf{d}_1$ lies along the LOS, and $\mathbf{d}_2$ is selected arbitrarily, the vector $\mathbf{d}_3$ thus is fixed once a choice for $\mathbf{d}_2$ is made. The interferometer frame $\mathcal{D}$, has an orientation with respect to the rotating frame $\mathcal{E}$, that is characterized by the EP set $\boldsymbol{\beta}_{D/E}$. An example of such a formation is shown in Figure 4.

The case in consideration assumes the mirror satellites are distributed over the surface of a sphere. However, modifications in the modeling can easily be made for aspherical formations by using parametric representations of the surfaces. Each satellite has associated with its position, a ring radius and a ring phase angle. The ring radius is determined by

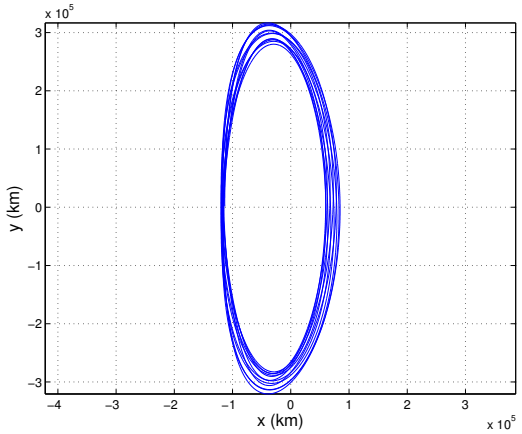

(i) Projection of Orbit in X-Y Plane

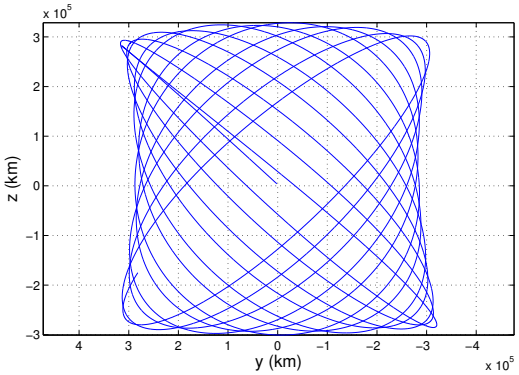

(ii) Projection of Orbit in Y-Z Plane

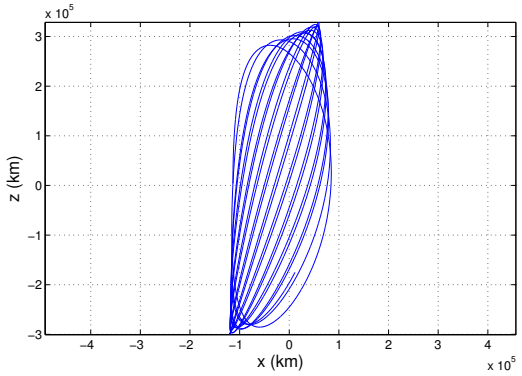

(iii) Projection of Orbit in X-Z Plane

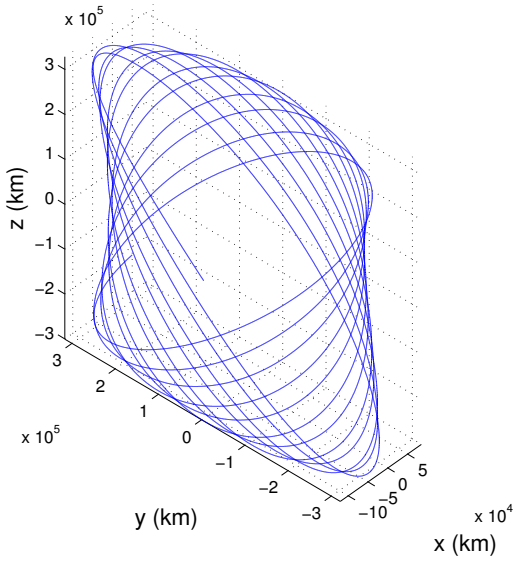

(iv) 3D Representation of Lissajous Orbit

Figure 3. Numerically Generated Lissajous Orbit

the distance of the ring from the focal satellite (since it is constrained to lie on the sphere). Thus, the position of the ith mirror satellite in the $\mathcal{D}$ frame is given by the vector

$$\mathbf{r}_{D_i} = d_i\mathbf{d}_1 + r_i\cos(\alpha_{0_i} + \dot{\alpha}t)\mathbf{d}_2 + r_i\sin(\alpha_{0_i} + \dot{\alpha}t)\mathbf{d}_3 \tag{16}$$

where d_i is the distance of the ring of ith satellite from the origin, and r_i and α_{0_i} are respectively the ring radius and phase angle associated with the ith satellite. The rotation of the formation about the LOS vector is introduced via the term $\dot{\alpha}$.

The interferometer has two operational modes of interest:

1. Inertial pointing in this case the line-of-sight (LOS) vector of the interferometer is fixed inertially (e.g. observation of a galaxy or a star), and the formation rotates

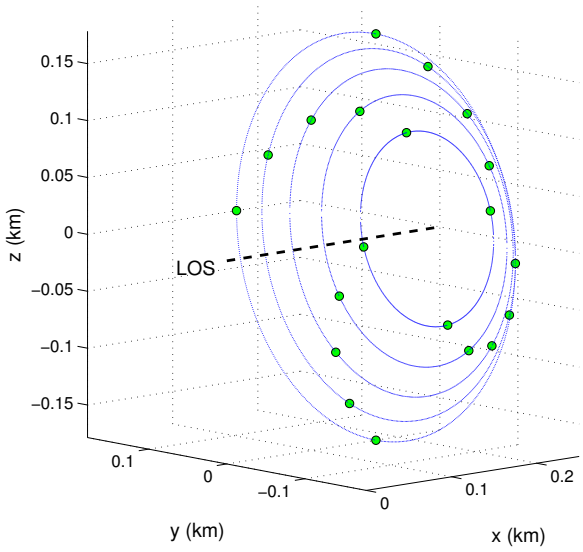

Figure 4. Sample Formation for Interferometer

with respect to the rotating frame and the line joining the Sun to the Earth-Moon barycenter. A feedback law uses continuous control for station-keeping. Furthermore, the treatment of the satellite as a rigid body also yields the problem of individual pointing of each satellite. This is handled by the use of a Lyapunov-based feedback scheme, that orients each satellite in the desired direction. In this case, attitude control has to take into account gravitational effects (apart from rigid body gyroscopic effects). Attitude control is performed by the use of momentum wheels on the satellite.

2. LVLH pointing in this case, the LOS is fixed in the rotating frame (e.g. solar or terrestrial observation. The attitude control has to account for gravitational as well as eccentricity effects, since the rotation of the frame is not constant in the ER3BP.

Slewing maneuvers are easily performed due to the feedback nature of the control laws derived for control: the formation has to re-stabilize itself about a new LOS vector, and the same control law can be used for formation maintenance as well as formation slewing.

CONTROL REQUIREMENT HOMOGENIZATION VIA FORMATION ROTATION

The concept of formation rotation as a means of fuel consumption homogenization has been utilized very successfully for formations in orbit around the Earth.[19] Vadali et al.[11] have also applied fuel balancing to circular formations in halo orbits. It is shown that for some cases, formation rotation actually reduces the total amount of control required for the stationkeeping in a mission. To gain insight into the problem, it is assumed in this paper that the focal satellite lies on the nominal trajectory that exactly satisfies Eq. (6), and therefore requires negligible control for station keeping. Let the state vector of the focal satellite be $\mathbf{x}_f$. The position of a mirror satellite, relative to that of the focus, is given by

$(\overline{x},\ \overline{y},\ \overline{z})$. Thus, the position of the mirror satellite in the coordinate frame at L_2, is given by $(x_f+\overline{x},\ y_f+\overline{y},\ z_f+\overline{z})$. A first approximation for the control required to maintain the mirror satellite along this trajectory is obtained by replacing this trajectory into a linearized form of Eq. (6), given by:

$$\ddot{x} - 2\dot{y} - (1+2B_L)x = 0 \tag{17a}$$
$$\ddot{y} + 2\dot{x} + (B_L - 1)y = 0 \tag{17b}$$
$$\ddot{z} + B_L z = 0 \tag{17c}$$

where B_L is a coefficient arising from the Legendre polynomial approximation of the gravitational potential, taking the following form:

$$B_L = \frac{(1-\mu)}{(1+\gamma_L)^3} + \frac{\mu}{\gamma_L^3} \tag{18}$$

Therefore,

$$u_x = \ddot{\overline{x}} - 2\dot{\overline{y}} - (1+2B_L)\overline{x} \tag{19a}$$
$$u_y = \ddot{\overline{y}} + 2\dot{\overline{x}} + (B_L - 1)\overline{y} \tag{19b}$$
$$u_z = \ddot{\overline{z}} + B_L\overline{z} \tag{19c}$$

If it is desired that the mirror satellite travel in a circle of radius R relative to the focal satellite, then

$$\begin{Bmatrix} \overline{x} \\ \overline{y} \\ \overline{z} \end{Bmatrix} = \begin{bmatrix} 1 & 0 & 0 \\ 0 & \cos\alpha & -\sin\alpha \\ 0 & \sin\alpha & \cos\alpha \end{bmatrix} \begin{Bmatrix} 0 \\ R \\ 0 \end{Bmatrix} \tag{20}$$

The optimal rate of rotation of this formation is sought, if the plane of rotation is also rotated about $\mathbf{e}_3$. For example, if the formation is required to look in a specific inertial direction, the rate of rotation about $\mathbf{e}_3$ is -1. To this end, let the current angle of the formation plane with respect to the the Y-Z plane be β. Then the relative position of the mirror satellite evolves as:

$$\begin{Bmatrix} \overline{x} \\ \overline{y} \\ \overline{z} \end{Bmatrix} = \begin{bmatrix} \cos\beta & \sin\beta & 0 \\ -\sin\beta & \cos\beta & 0 \\ 0 & 0 & 1 \end{bmatrix} \begin{bmatrix} 1 & 0 & 0 \\ 0 & \cos\alpha & -\sin\alpha \\ 0 & \sin\alpha & \cos\alpha \end{bmatrix} \begin{Bmatrix} 0 \\ R \\ 0 \end{Bmatrix} \tag{21}$$

or,

$$\begin{aligned} \overline{x} &= R\cos\alpha\sin\beta \\ \overline{y} &= R\cos\alpha\cos\beta \\ \overline{z} &= R\sin\alpha \end{aligned} \tag{22a}$$

$$\begin{aligned} \dot{\overline{x}} &= -R\dot{\alpha}\sin\alpha\sin\beta + R\dot{\beta}\cos\alpha\cos\beta \\ \dot{\overline{y}} &= -R\dot{\alpha}\sin\alpha\cos\beta - R\dot{\beta}\cos\alpha\sin\beta \\ \dot{\overline{z}} &= R\dot{\alpha}\cos\alpha \end{aligned} \tag{22b}$$

$$\begin{aligned} \ddot{\overline{x}} &= -R(\dot{\alpha}^2+\dot{\beta}^2)\cos\alpha\sin\beta - 2R\dot{\alpha}\dot{\beta}\sin\alpha\cos\beta \\ \ddot{\overline{y}} &= -R(\dot{\alpha}^2+\dot{\beta}^2)\cos\alpha\cos\beta + 2R\dot{\alpha}\dot{\beta}\sin\alpha\sin\beta \\ \ddot{\overline{z}} &= -R\dot{\alpha}^2\sin\alpha \end{aligned} \tag{22c}$$

where, $\alpha = \alpha_0 + \dot{\alpha}t$ and $\beta = \dot{\beta}t$. For a given rate of planar rotation, it can be shown that the average control requirement for the rotation of an infinite number of satellites in a circle, is of the following form:

$$\begin{aligned} u_{avg} &= \frac{1}{2\pi}\int_0^{2\pi}\int_0^{2\pi}(u_x^2 + u_y^2 + u_z^2)\; dt\; d\alpha_0 \\ &= A\dot{\alpha}^4 + B\dot{\alpha}^2 + C \end{aligned} \tag{23}$$

with,

$$A = 2\pi R^2, \qquad B = \pi R^2\left[6\dot{\beta}(\dot{\beta}-2) - B_L + 6 - 3B_L\frac{\sin 4\pi\dot{\beta}}{4\pi\dot{\beta}}\right] \tag{24}$$

The value of C is lengthy, and is not required in the analysis here. The minimum control requirement is obtained when:

$$\dot{\alpha} = 0,\; \pm\left(-\frac{B}{2A}\right)^{\frac{1}{2}}$$

The value $\dot{\alpha} = 0$ corresponds to a local maxima, and the other two values correspond to minima. Thus, the characteristics of the following expression are of interest:

$$\dot{\alpha}_{\text{opt}} = \frac{1}{2}\left[B_L - 6 + 3B_L\frac{\sin 4\pi\dot{\beta}}{4\pi\dot{\beta}} - 6\dot{\beta}(\dot{\beta}-2)\right]^{\frac{1}{2}} \tag{25}$$

In the limit $\dot{\beta} \to 0$, Eq. (25) reduces to[‡]:

$$\dot{\alpha}_{\text{opt}} = \pm\frac{1}{2}\left(4B_L - 6\right)^{\frac{1}{2}} \tag{26}$$

It should be noted that an optimal value of $\dot{\alpha}$ will only exist, when

$$6\dot{\beta}(\dot{\beta}-2) - B_L + 6 - 3B_L\frac{\sin 4\pi\dot{\beta}}{4\pi\dot{\beta}} < 0 \tag{27}$$

Figure 5(i) shows the optimal rate of formation rotation, for varying $\dot{\beta}$. In the cases where $B > 0$, the only real root for the optimal $\dot{\alpha}$ is zero. This occurs, for example, in the case of inertial pointing, with $\dot{\beta} = -1$.

[‡]A similar analysis accounting for first-order eccentricity terms leads to the use of the following expressions:

$$\begin{aligned} &\ddot{x} - (2 + 4e\cos t)\dot{y} - [(1 + 2B_L) + 2e(2 + 3B_L)\cos t]\, x + 2e\sin t y = 0 \\ &\ddot{y} + (2 + 4e\cos t)\dot{x} - [(1 - B_L) + e(4 - 3B_L)\cos t]\, y - 2e\sin t x = 0 \\ &\ddot{z} + (1 + 3e\cos t)B_L z = 0 \end{aligned}$$

Yielding,

$$\dot{\alpha}_{\text{opt}} = \frac{1}{2}\left[4B_L - 6 - 8e^2\right]^{\frac{1}{2}}$$

Using $\sin x \approx x - x^3/3!$, Eq. (27) yields a quadratic inequality, which can be solved to obtain the range in which $B \leq 0$. The limits of this range of values of $\dot{\beta}$ can be obtained by solving for the roots of the following equation:

$$(8B_L\pi^2 + 6)\dot{\beta}^2 - 12\dot{\beta} - (4B_L - 6) = 0 \tag{28}$$

This yields $\dot{\beta}_{\min} \approx -0.16$, and $\dot{\beta}_{\max} \approx 0.20$.

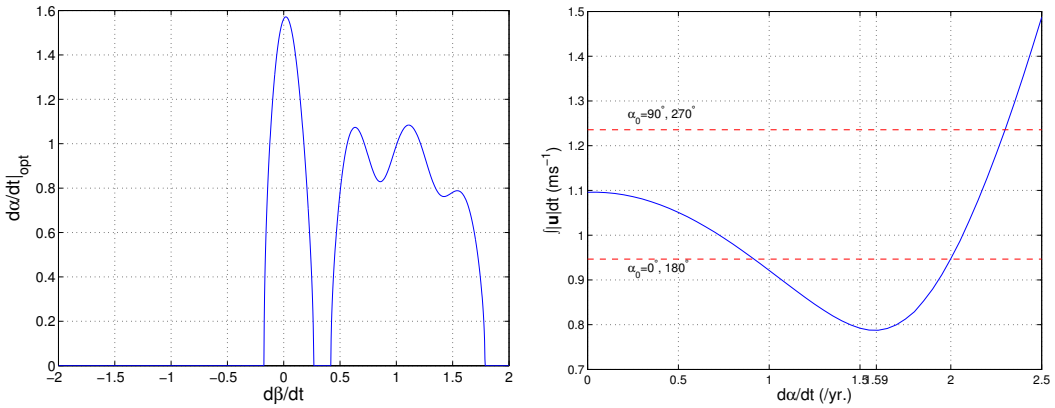

(i) Variation of $\dot{\alpha}_{\text{opt}}$ with $\dot{\beta}$

(ii) Effect of Formation Rotation on Control Requirement

Figure 5. Formation Rotation

If the formation does not rotate about $\mathbf{e}_3$, then numerical simulations show that the optimal rate of formation rotation agrees with the rate predicted in Eq. (26). This is shown for a Lissajous trajectory with $A_y = A_z = 300,000$km, in Figure 5(ii). The dashed lines indicate the control requirement for individual satellites placed at phase angles 0°, 90°, 180° and 270°. The solid line indicates the average control requirement if all four satellites are rotated, for varying $\dot{\alpha}$. In this case, the predicted value of $\dot{\alpha}_{\text{opt}}$ is 1.56, whereas the value obtained from numerical simulations is 1.59. In dimensional terms, this is approximately once every 9 months. Intuitively, it would be expected that an optimal value for rotating the formation would be approximately 6 months, to match with the Lissajous orbit period. However, from Figure 5(i), it is observed that $\dot{\alpha}_{\text{opt}} = 2$ is not an optimal value for any value of $\dot{\beta}$. Thus, no relation to the Lissajous orbit period is evident.

In the analysis in this section, the equations of motion have been linearized with respect to the L_2 point. This is a possible explanation for the difference between analytical and numerically obtained optimal rates of rotation. More accurate results can be obtained if the equations of the mirror satellite are linearized with respect to the focal satellite.[20] However, this leads to a linear equation with periodic coefficients that depend on the states of the focal satellite. Either an approximate trajectory for the Lissajous orbit for the focal satellite may be used, or the numerical values for its states can be used to evaluate te optimal rate of formation rotation. In fact, the latter defeats the purpose of the analysis in this section. To reduce the complexity of calculations, this paper uses linearized motion about the L_2 point only.

Fuel balancing via formation rotation ceases to be of use when either of the following cases:

1. Faster rotation rates - depending on mission requirements, one rotation every 9 months may be too slow.
2. Rotation of the formation about the axis normal to the Sun-Earth plane - in this case, as is shown in Figure 5(i), the formation is best left stationary.

INTERFEROMETER FORMATION-KEEPING

While the focal satellite requires very little control to remain on the Lissajous trajectory, the mirror satellites will require control, since their trajectories are not natural solutions to Eq. (6). In this section, the control requirement for formation keeping for various configurations are explored. The numerical method used to obtain Lissajous trajectories generates target points roughly 10 days apart. A quintic polynomial is used a spline, to maintain continuity at the position, velocity, and acceleration levels.

Let the current position of the ith satellite be $\mathbf{r}_i$. A Lyapunov function for each satellite, $V_i : \mathbb{R}^6 \mapsto \mathbb{R}$, is defined as follows:

$$V_i = \frac{1}{2}(\mathbf{r}_i - \mathbf{r}_{\mathrm{des}_i})^T(\mathbf{r}_i - \mathbf{r}_{\mathrm{des}_i}) + \frac{1}{2}(\dot{\mathbf{r}}_i - \dot{\mathbf{r}}_{\mathrm{des}_i})^T\mathbf{K}_i(\dot{\mathbf{r}}_i - \dot{\mathbf{r}}_{\mathrm{des}_i}) \tag{29}$$

where $\mathbf{K}_i \in \mathbb{R}^{3\times3}$ is positive definite. The function $\mathbf{r}_{\mathrm{des}_i}$ is a piecewise continuous representation of the reference trajectory, of the following form:

$$\begin{aligned} \mathbf{r}_{\mathrm{des_i}} &= \mathbf{r}_{E_i} + \mathbf{r}_{\mathrm{qs}} \\ \mathbf{r}_{\mathrm{qs}} &= \mathbf{p}_{j_0} + \mathbf{p}_{j_1}t + \mathbf{p}_{j_2}t^2 + \mathbf{p}_{j_3}t^3 + \mathbf{p}_{j_4}t^4 + \mathbf{p}_{j_5}t^5 \quad \forall t \in [t_{j_0}, t_{j_f}] \end{aligned} \tag{30}$$

where $\mathbf{r}_{E_i}$ is the position of the ith satellite in the $\mathcal{E}$ frame. It is immediately obvious that V_i is positive definite everywhere except on the desired trajectory. By defining $\overline{\mathbf{K}}_i \in \mathbb{R}^{3\times3}$, it is also easy to show that a control, $\mathbf{u}_i \in U \subset \mathbb{R}^3$ renders $\dot{V}_i$ negative definite everywhere except on the desired trajectory:

$$\mathbf{u}_i = \ddot{\mathbf{r}}_{\mathrm{des}_i} - \mathbf{f}(\mathbf{r}_i, \dot{\mathbf{r}}_i) - \mathbf{L}_i(\dot{\mathbf{r}}_i - \dot{\mathbf{r}}_{\mathrm{des}_i}) - \overline{\mathbf{L}}_i(\mathbf{r}_i - \mathbf{r}_{\mathrm{des}_i}) \tag{31}$$

where $\mathbf{L}_i = \mathbf{K}_i^{-1}\overline{\mathbf{K}}_i$ and $\overline{\mathbf{L}}_i = \mathbf{K}_i^{-1}$. Thus $\mathbf{u}_i$ is a globally, asymptotic stabilizing controller.

Formation-Keeping for LVLH Pointing

For the interferometer to have LVLH pointing, $\mathcal{D}$ must have a constant orientation with respect to $\mathcal{E}$, i.e., the desired EP set, $\boldsymbol{\beta}_{D/E_{\mathrm{des}}}$ is given and constant. Using Eq. (16), the position of the ith mirror in the basis corresponding to $\mathcal{E}$ is thus:

$$\mathbf{r}_{E_i} = \mathbf{C}^T_{D/E_{\mathrm{des}}}\mathbf{r}_{D_i} \tag{32a}$$

$$\text{Consequently,} \quad \dot{\mathbf{r}}_{E_i} = \mathbf{C}^T_{D/E_{\mathrm{des}}}\dot{\mathbf{r}}_{D_i} \tag{32b}$$

$$\ddot{\mathbf{r}}_{E_i} = \mathbf{C}^T_{D/E_{\mathrm{des}}}\ddot{\mathbf{r}}_{D_i} \tag{32c}$$

since the direction cosine matrix $\mathbf{C}_{D/E_{\rm des}} \equiv \mathbf{C}_{D/E_{\rm des}}(\boldsymbol{\beta}_{D/E_{\rm des}})$ is constant. The time derivatives of $\mathbf{r}_{D_i}$ are local in the $\mathcal{D}$ frame; therefore:

$$\dot{\mathbf{r}}_{D_i} = -r_i\dot{\alpha}\sin(\alpha_{0_i}+\dot{\alpha}t)\mathbf{d}_2 + r_i\dot{\alpha}\cos(\alpha_{0_i}+\dot{\alpha}t)\mathbf{d}_3 \quad (33a)$$

$$\ddot{\mathbf{r}}_{D_i} = -r_i\dot{\alpha}^2\cos(\alpha_{0_i}+\dot{\alpha}t)\mathbf{d}_2 - r_i\dot{\alpha}^2\sin(\alpha_{0_i}+\dot{\alpha}t)\mathbf{d}_3 \quad (33b)$$

Equations (32) and (33) are used with Eq. (30) to generate a control law from Eq. (31).

Formation-Keeping for Inertial Pointing

If a constant inertial pointing is desired, then the EP set, $\boldsymbol{\beta}_D$ that orients $\mathcal{D}$ with $\mathcal{N}$ is constant, i.e., $\boldsymbol{\beta}_{D/E_{\rm des}}$ is no longer constant. It follows that:

$$\dot{\mathbf{r}}_{E_i} = \mathbf{C}^T_{D/E_{\rm des}}(\dot{\mathbf{r}}_{D_i} + \widetilde{\boldsymbol{\omega}}_{D/E_{\rm des}}\mathbf{r}_{D_i}) \quad (34a)$$

$$\ddot{\mathbf{r}}_{E_i} = \mathbf{C}^T_{D/E_{\rm des}}(\ddot{\mathbf{r}}_{D_i} + \dot{\widetilde{\boldsymbol{\omega}}}_{D/E_{\rm des}}\mathbf{r}_{D_i} + 2\widetilde{\boldsymbol{\omega}}_{D/E_{\rm des}}\dot{\mathbf{r}}_{D_i} + \widetilde{\boldsymbol{\omega}}_{D/E_{\rm des}}\widetilde{\boldsymbol{\omega}}_{D/E_{\rm des}}\mathbf{r}_{D_i}) \quad (34b)$$

Since the interferometer is fixed inertially, the inertial angular velocity $\boldsymbol{\omega}_D = 0$. Furthermore, the desired angular velocity of the frame is $\boldsymbol{\omega}_{E_{\rm des}} = (1+\nu)\mathbf{e}_3$, and it follows that the relative angular velocity between $\mathcal{D}$ and $\mathcal{E}$, expressed in $\mathcal{D}$, is:

$$\boldsymbol{\omega}_{D/E_{\rm des}} = -(1+\nu)\mathbf{c}_{D/E\mathrm{des}_3} \quad (35a)$$

$$\text{Consequently,}\quad \dot{\boldsymbol{\omega}}_{D/E_{\rm des}} = \left[-\dot{\nu}\mathbb{1} + (1+\nu)\widetilde{\boldsymbol{\omega}}_{D/E}\right]\mathbf{c}_{D/E\mathrm{des}_3} \quad (35b)$$

where $\mathbf{c}_{D/E\mathrm{des}_3}$ is the third column of $\mathbf{C}_{D/E_{\rm des}}$. Since $\boldsymbol{\beta}_{D_{\rm des}}$ is fixed and $\boldsymbol{\beta}_E = \{\cos\theta/2\ 0\ 0\ \sin\theta/2\}^T$, $\boldsymbol{\beta}_{D/E_{\rm des}}$ is given by an expression similar to Eq. (13).

ATTITUDE CONTROL FOR THE MIRROR SATELLITES

Attention is now focused on the problem of attitude control. If the interferometry assembly is small in comparison with the astronomical distances, it is sufficient to demonstrate the attitude control on one satellite (viz., the focal satellite), since they are all required to have the same orientation, and the disturbance torques acting on all satellites are of the same order. Control laws to maintain orientation of the general rigid spacecraft with an arbitrary number of momentum wheels, in the desired direction are presented in this section.

Attitude Control for LVLH Pointing

The desired attitude of the spacecraft is assumed to be the same as that of the interferometer frame. For LVLH pointing, therefore, $\boldsymbol{\beta}_{B/E_{\rm des}}$ is given and constant. Let $\boldsymbol{\beta}_{B/E}$ characterize the current orientation of the satellite frame $\mathcal{B}$ with respect to the rotating frame $\mathcal{E}$. The error EP set is thus defined as the relative orientation between the current and desired EPs, i.e.,

$$\boldsymbol{\Delta\beta} = \begin{bmatrix} \beta_{B/E_{\mathrm{des}_0}} & \beta_{B/E_{\mathrm{des}_1}} & \beta_{B/E_{\mathrm{des}_2}} & \beta_{B/E_{\mathrm{des}_3}} \\ -\beta_{B/E_{\mathrm{des}_1}} & \beta_{B/E_{\mathrm{des}_0}} & \beta_{B/E_{\mathrm{des}_3}} & -\beta_{B/E_{\mathrm{des}_2}} \\ -\beta_{B/E_{\mathrm{des}_2}} & -\beta_{B/E_{\mathrm{des}_3}} & \beta_{B/E_{\mathrm{des}_0}} & \beta_{B/E_{\mathrm{des}_1}} \\ -\beta_{B/E_{\mathrm{des}_3}} & \beta_{B/E_{\mathrm{des}_2}} & -\beta_{B/E_{\mathrm{des}_1}} & \beta_{B/E_{\mathrm{des}_0}} \end{bmatrix} \boldsymbol{\beta}_{B/E} \quad (36)$$

The matrix in the above expression is constant. Therefore, $\boldsymbol{\Delta\dot{\beta}} = [\cdot]\,\dot{\boldsymbol{\beta}}_{D/E}$. It is also desired that the satellite be brought to rest with respect to the rotating frame, at equilibrium; therefore, $\boldsymbol{\omega}_{B/E} = \boldsymbol{\omega}_B - \mathbf{C}_{B/E}\boldsymbol{\omega}_E \to 0$.

Let $\mathbf{z} = \left\{\boldsymbol{\Delta\beta}^T \quad \boldsymbol{\omega}_{B/E}^T\right\}^T$ be a state vector such that $\mathbf{z} \in S^3 \times Z$ where S^3 is the 3-sphere, and $Z \subset \mathbb{R}^3$; and $\overline{\mathbf{u}} \in U$ where $U \subset \mathbb{R}^3$. Then, the Lyapunov function, $V_1 : S^3 \times Z \mapsto \mathbb{R}$ is defined as

$$V_1(\mathbf{z}) = (1 - \Delta\beta_0)^2 + \widetilde{\boldsymbol{\Delta\beta}}^T\widetilde{\boldsymbol{\Delta\beta}} + \frac{1}{2}\boldsymbol{\omega}_{B/E}^T\mathbf{K}_1\boldsymbol{\omega}_{B/E} \tag{37}$$

where $\mathbf{K}_1 \in \mathbb{R}^{3\times3}$ is positive definite, and $\widetilde{\boldsymbol{\Delta\beta}}$ denotes the reduced EP set, $\Delta\beta_i$, $i = 1\ldots3$. When the desired orientation is achieved, $\Delta\beta_0 = 1$ and $\widetilde{\boldsymbol{\Delta\beta}} = \boldsymbol{\omega}_{B/E} = \mathbf{0}$, so it is evident that V_1 is positive definite every except at equilibrium. Taking the time derivative of V_1, it can be shown that

$$\dot{V}_1 = \boldsymbol{\omega}_{B/E}^T\left[\widetilde{\boldsymbol{\Delta\beta}} + K_1\dot{\boldsymbol{\omega}}_{B/E}\right] \tag{38}$$

To make $\dot{V}_1$ negative definite, Eqs. (9) are substituted in Eq. (38) to obtain the following control law:

$$\begin{aligned}
\overline{\mathbf{u}} &= -\widetilde{\overline{\boldsymbol{\omega}}}\left(\overline{\mathbf{I}}\overline{\boldsymbol{\omega}} + \overline{\mathbf{h}}\right) + \boldsymbol{\tau}_d + \left(\overline{\mathbf{I}} - \overline{\mathbf{Q}}\mathbf{J}_a\overline{\mathbf{Q}}^T\right)\left(\mathbf{L}_1\boldsymbol{\omega}_{B/E} + \mathbf{L}_2\widetilde{\boldsymbol{\Delta\beta}} - \dot{\overline{\boldsymbol{\omega}}}\right) \\
\dot{\overline{\boldsymbol{\omega}}} &= \mathbf{C}_{B/E}\left\{\begin{array}{c} 0 \\ 0 \\ \dot{\nu} \end{array}\right\} - \widetilde{\boldsymbol{\omega}}_{B/E}\left\{\begin{array}{c} 0 \\ 0 \\ 1+\nu \end{array}\right\}
\end{aligned} \tag{39}$$

where, $\mathbf{L}_2 \in \mathbb{R}^{3\times3}$ is also positive definite, $\mathbf{L}_1 = \mathbf{K}_1^{-1}\mathbf{K}_2$, and $\mathbf{L}_2 = \mathbf{K}_1^{-1}$. Upon substitution of Eq. (39) in Eqs. (38),

$$\dot{V}_1 = -\boldsymbol{\omega}_{B/E}^T\mathbf{K}_2\boldsymbol{\omega}_{B/E} \tag{40}$$

Furthermore, substitution of Eq. (39) in Eqs. (38) yields the following system of equations:

$$\dot{\boldsymbol{\omega}}_{B/E} + \mathbf{L}_1\boldsymbol{\omega}_{B/E} + \mathbf{L}_2\widetilde{\boldsymbol{\Delta\beta}} = \mathbf{0} \tag{41}$$

If $\boldsymbol{\omega}_{B/E} = 0$, then $\dot{\boldsymbol{\omega}}_{B/E} = 0$ and it follows from the above equation that $\widetilde{\boldsymbol{\Delta\beta}} = \mathbf{0}$, or $\boldsymbol{\Delta\beta} = \{1 \quad 0 \quad 0 \quad 0\}^T$. Thus from Eq. (40) and Eq. (41), $\dot{V}_1$ is zero at the equilibrium only, proving that the control defined in Eq. (39) asymptotically stabilizes the system about the desired equilibrium.

Attitude Control for Inertial Pointing

If it is desired to keep the spacecraft fixed in a desired direction in the inertial frame, then $\boldsymbol{\beta}_{B_{\text{des}}}$ is given and constant. From Eq. (13),

$$\boldsymbol{\Delta\beta} = \begin{bmatrix} \beta_{B_0} & \beta_{B_1} & \beta_{B_2} & \beta_{B_3} \\ \beta_{B_1} & -\beta_{B_0} & -\beta_{B_3} & \beta_{B_2} \\ \beta_{B_2} & \beta_{B_3} & -\beta_{B_0} & -\beta_{B_1} \\ \beta_{B_3} & -\beta_{B_2} & \beta_{B_1} & -\beta_{B_0} \end{bmatrix}\boldsymbol{\beta}_{B_{\text{des}}} \tag{42}$$

Furthermore, it is desired that $\boldsymbol{\omega} \to 0$.

The Lyapunov function is of a similar structure as in the previous case. Let $\mathbf{z} = \left\{\boldsymbol{\Delta\beta}^T \quad \boldsymbol{\omega}^T\right\}^T$ be a state vector such that $\mathbf{z} \in S^3 \times Z$ where S^3 is the 3-sphere, and $Z \subset \mathbb{R}^3$; and $\overline{\mathbf{u}} \in U$ where $U \subset \mathbb{R}^3$. Then, the Lyapunov function, $V_2 : S^3 \times Z \mapsto \mathbb{R}$ is defined as

$$V_2(\mathbf{z}) = (1 - \Delta\beta_0)^2 + \widetilde{\boldsymbol{\Delta\beta}}^T \widetilde{\boldsymbol{\Delta\beta}} + \frac{1}{2}\boldsymbol{\omega}^T \mathbf{K}_3 \boldsymbol{\omega} \tag{43}$$

where $\mathbf{K}_3 \in \mathbb{R}^{3\times3}$ is positive definite. It is again evident that V_2 is positive definite every except at equilibrium. Taking the time derivative of V_2,

$$\dot{V}_2 = \boldsymbol{\omega}^T \left[\widetilde{\boldsymbol{\Delta\beta}} + \mathbf{K}_3 \dot{\boldsymbol{\omega}}\right] \tag{44}$$

Again, to make $\dot{V}$ negative definite, Eqs. (9) are substituted in Eq. (44) to obtain the following control law:

$$\overline{\mathbf{u}} = -\widetilde{\boldsymbol{\omega}}\left(\overline{\mathbf{I}}\boldsymbol{\omega} + \overline{\mathbf{h}}\right) + \boldsymbol{\tau}_d + \left(\overline{\mathbf{I}} + \overline{\mathbf{Q}}\mathbf{J}_a\overline{\mathbf{Q}}^T\right)\left(\mathbf{L}_3\boldsymbol{\omega} + \mathbf{L}_4\widetilde{\boldsymbol{\Delta\beta}}\right) \tag{45}$$

where $\mathbf{L}_3 = \mathbf{K}_3^{-1}\mathbf{K}_4$, $\mathbf{L}_4 = \mathbf{K}_3^{-1}$, and $\mathbf{K}_4 \in \mathbb{R}^{3\times3}$ is positive definite. The control law in Eq. (45) can also be shown to be asymptotically stable by the use of LaSalle's theorem.

NUMERICAL SIMULATIONS

In this section, a sample configuration for a Fizeau interferometer is introduced and control requirements for stationkeeping and attitude maintenance for the operational modes are calculated. In the example considered, the mirror satellites are distributed over a sphere of radius 250m, the center of which is 100km away from the focal satellite, along the LOS vector. The 20 mirror satellites are assumed to be evenly distributed over 5 rings. The 4 rings on each satellite are placed 90° apart from each other, and the satellites on each ring are staggered by 18° for uniform coverage, as shown in Figure 4. The positions of the rings are given by:

$$d_i = -100 - \{0.175 \quad -0.190 \quad -0.205 \quad -0.220 \quad -0.235\}\,\text{km} \tag{46}$$

The formation may be rotated at any desired rate in the case of inertial pointing, since it has been established that no optimal rate of rotation exists.

The satellite is modeled with three identical momentum wheels along its principal axes. The following values for the moments of inertia of the satellite and momentum wheels are selected:

$$I_1 = 5000\text{kgm}^2 \quad I_2 = 10000\text{kgm}^2 \quad I_3 = 12000\text{kgm}^2 \quad J_a = 0.6\text{kgm}^2 \quad J_t = 0.001\text{kgm}^2$$

If the wheels are aligned with the principal axes of the satellite and their distance from the center of mass of the spacecraft is assumed negligible, then the following are true:

$$\mathbf{h}, \overline{\mathbf{h}}, \mathbf{u}, \overline{\mathbf{u}} \in \mathbb{R}^3$$

$$\overline{\mathbf{Q}} = \mathbb{1}$$
$$\mathbf{J}_a = J_a \mathbb{1}$$
$$\overline{I}_i = I_i + 2J_t, i = 1 \ldots 3$$

The effective SRP area of the satellite is taken to be 20m^2, and the center of the pressure is located at $(0.2\mathbf{b}_2 + 0.1\mathbf{b}_3)$m. The coefficients $\rho_s = 0.05$, $\rho_a = 0.8$, and $\rho_d = 0.15$. For the sake of simplicity, the gains selected for attitude control are of the form $\mathbf{L}_i = l_i \mathbb{1}$. The values l_i are selected such that the closed-loop dynamics have high frequency and critical damping. This is necessary so that slewing maneuvers are performed in a matter of days instead of months, and the desired pointing is attained in an exponential fashion. Consequently, $l_2, l_4 > 10^4$ and $l_1 = 2\sqrt{l_2}, \quad l_3 = 2\sqrt{l_4}$. The gains for translational control are taken as the identity matrices since this paper does not consider formation establishment.

Translation Control

The control requirement for translational motion is measured by integrating the norm of the control, and compared in terms of the Δv-equivalent. That is, $J = \int_0^t |\mathbf{u}| \, dt$.

The Δv for a desired pointing of $\boldsymbol{\beta}_{D/E_{\text{des}}} = \{0 \quad 0 \quad 0 \quad 1\}^T$ (constant pointing along the Sun-Earth/Moon line) is shown in Figure 6(i). The Δv varies from 0.5m/s/yr for the first (closest) ring, to 0.46m/s/yr for the fifth (farthest) ring. For an inertial pointing

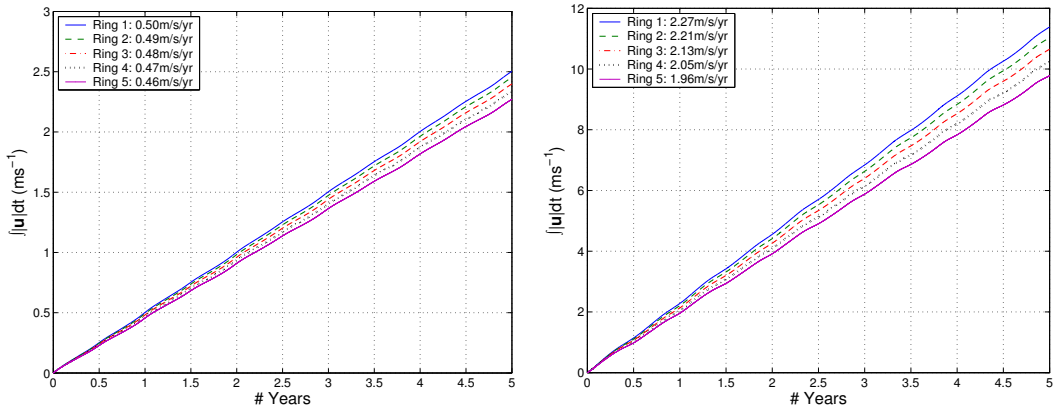

(i) LVLH Pointing **(ii)** Inertial Pointing

Figure 6. Δv for Desired Operational Modes

of $\beta_{D_{\text{des}}} = \{0 \quad 0 \quad 0 \quad 1\}^T$, the formation-keeping Δv is shown in Figure 6(ii). The Δv for inertial pointing varies from 2.27m/s/yr for the innermost ring to 1.96m/s/yr for the outermost ring. It is observed that the Δv for inertial pointing is more than the Δv for LVLH pointing. This is a direct consequence of the constant slewing that is occuring to keep the formation fixed inertially. The base Δv for keeping the formation on the Lissajous trajectory are of the order of 0.025-0.030m/s/yr with the use of the quintic splines. In both cases, the force due to SRP is negligible in comparison with gravitational forces.

Attitude Control

For a satellite with the inertia and SRP properties selected as above, the SRP torque is of the order of 10^{-5}Nm and the gravity-gradient torque is of the the order of 10^{-9}Nm. The motor torques required for LVLH pointing in the orientation selected above, are shown in Figure 7(i). It is observed that the motor torque in the $\mathbf{b}_3$ axis is almost constant while the other two vary periodically; this is because the orientation of the Sun with respect to the mirrors is fixed, and for the desired orientation studied, no rotation about the $\mathbf{e}_3/\mathbf{b}_3$ axis is required. Assuming a fixed torque of 2.2×10^{-5}Nm, a trivial calculation for the wheel angular velocity in the $\mathbf{b}_3$ direction shows that $\dot{\Omega}_3 = (2.2 \times 10^{-5}/0.6)$rad/s. Thus in 2 months, the wheel angular velocity is approximately 1815rpm. This can easily be observed from Figure 7(ii). Since the motor torques about the other two axes are periodic, the rpm profile of these wheels are also periodic. If the center of pressure is offset along $\mathbf{b}_1$ only, then the SRP torque is many magnitudes lower. Thus, by judicious design, control for SRP torque-negation can be minimized. Due to the constant nature of the torque from the wheel along $\mathbf{b}_3$, the rpm of that wheel, shown in Figure 7(ii), increases in an almost linear fashion. Since the rpm is certain to cross the threshold for momentum wheel design rpm, it is evident that momentum dumping must be performed periodically.

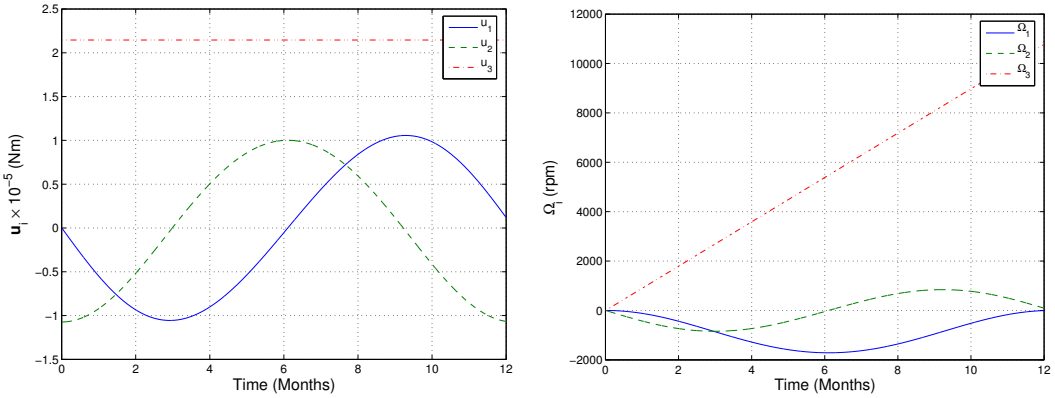

(i) Motor Torques for LVLH Pointing **(ii)** Wheel RPM

Figure 7. Control for LVLH Pointing

Figure 8(i) shows the motor torque for inertial pointing. It is observed that while the magnitude of the torque is of the same order as that required in LVLH pointing, the torque profile of all three motors is periodic in nature. This is because the satellite is fixed inertially, and therefore rotating with respect to the Sun about the $\mathbf{e}_3$ axis. The wheel rpm for this operation is shown in Figure 8(ii). Though the motor torques in Figure 8(i) appear periodic in nature, u_2 and u_3 do not have zero mean. This leads to secular growth in the corresponding wheel angular velocities. While they do not appear to grow at the same rate as that seen in LVLH pointing, some form of momentum management will be required to prevent saturation.

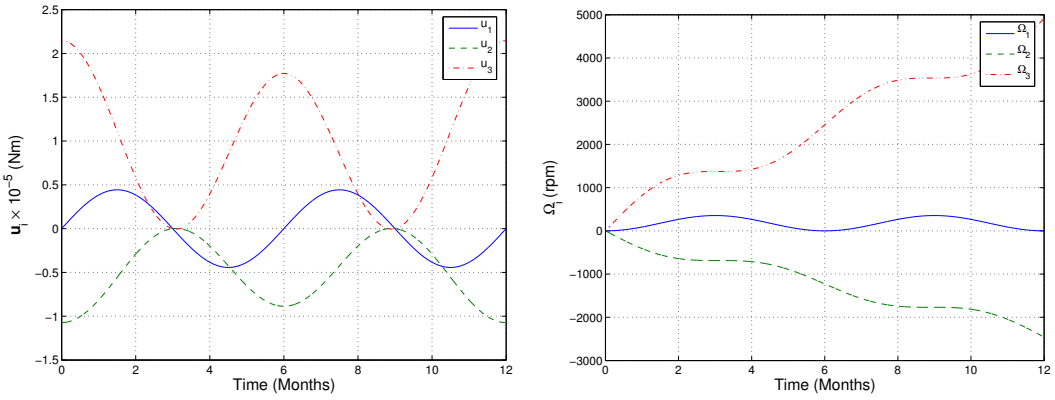

(i) Motor Torques for Inertial Pointing **(ii)** Wheel RPM

Figure 8. Control for Inertial Pointing

Effect of the Gravity-Gradient Torque

It has been observed that the gravity-gradient torque is many magnitudes smaller than the SRP torque. However, this torque cannot be ignored in the control formulation. To study its effects, the component of $\boldsymbol{\tau}_g$ appearing in $\boldsymbol{\tau}_d$ is ignored from the expressions for $\mathbf{u}$ in Eq. (39) and Eq. (45), but is present in the equations of motion in Eqs. (9). The excursion in pointing for the LVLH and inertial attitude maintenance are shown in Figure 9(i) and Figure 9(ii), respectively. In both cases, it is observed that the pointing error is periodic. If the SRP torque is also neglected in the control formulation, then growth in yaw, pitch, and roll pointing error (with respect to the desired LOS vector) is observed. In Figure 9(i), the error magnitudes are of the order of 10^{-5} deg. However, given the astronomical distances involved, this may mean very large errors in mission fulfilment. The errors involved in the inertial case, shown in Figure 9(ii) are of the order of 10^{-3} deg and are considerably higher.

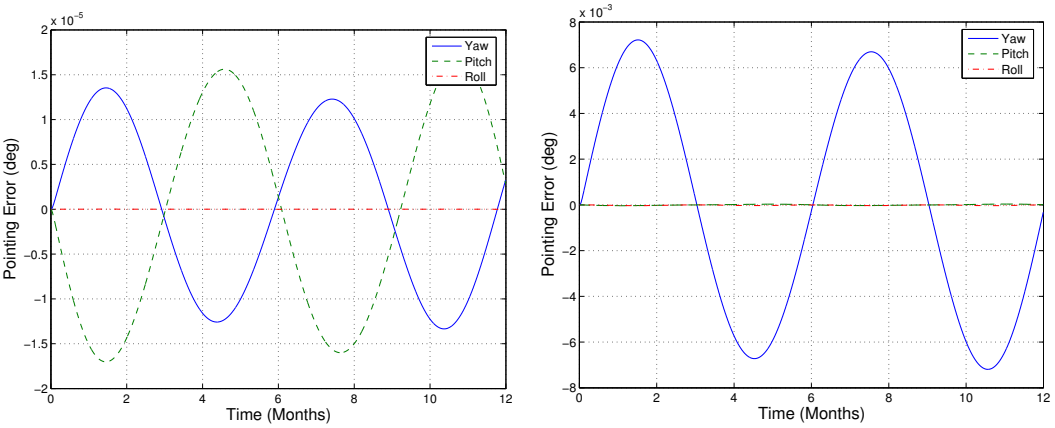

(i) LVLH Pointing **(ii)** Inertial Pointing

Figure 9. Pointing Excursion due to Gravity-Gradient Torque

Thus is it observed that though the magnitude of the gravity gradient-torque is small, it

is required to include its effects in control law formulation for high-fidelity missions such as the ones considered in this paper. It is also seen that using the wheel moments as specified, the typical rate of wheel rotations to control gravity-gradient torque are of orders < 0.1rpm. Therefore, some form of precision control is required for such missions.

CONCLUSIONS

A methodology for mission design of space-based interferometric systems around the libration points has been developed that takes into account combined translation and attitude kinematics of the spacecraft. Rigid body effects do not affect the translational motion of the satellite, but the translational motion of the satellite induces a gravity-gradient torque on it. Furthermore, solar radiation pressure is also included in the model, and its effects are studied.

The formation is placed on a nominal, accurate Lissajous orbit that takes into account the eccentricity of the Earth's orbit around the Sun. A stationkeeping methodology that uses quintic splines is used for continuous-control formation maintenance. A methodology is proposed that homogenizes the control requirement for all the satellites by rotating the formation at a particular rate. In some cases, this is shown to reduce the control requirement for stationkeeping.

Two operational modes of the interferometer are analyzed - inertial pointing, and LVLH pointing. Slewing maneuvers can easily be studied since the control law for inertial pointing can easily be extended to a form an inertial orientation about which slewing must stabilize the system. In both cases, the control requirement for formation-keeping is calculated. Control laws that are based on Lyapunov analysis yield algorithms to ensure that the attitude of the spacecraft does not deviate from the LOS vector due to gravitational and eccentricity effects.

One issue is the necessity of low-order thrust and attitude controls. These are required for accurate pointing; a small error in pointing angle leads to large errors in interferometric observations due to the astronomical distances involved. It should be noted that the exact thrusts required will, in general, vary due to the fact that the actuators themselves rotate with the satellite.

ACKNOWLEDGMENTS

This research was supported by Grant NCC5-737 under the NASA Cooperative Agreement. The authors wish to thank Richard Luquette for his valuable inputs and suggestions.

REFERENCES

1. "The International Sun-Earth/Cometary Explorer 3 Homepage," http://heasarc.gsfc.nasa.gov/docs/heasarc/missions/isee3.html.

2. "Stellar Imager Homepage," http://hires.gsfc.nasa.gov/∼si/.

3. "Terrestrial Planet Finder Homepage," http://planetquest.jpl.nasa.gov/TPF/tpf_index.html.

4. R. W. Farquhar, "The Control and Use of Libration-Point Satellites," Tech. Rep. NASA TR R-346, NASA Goddard Space Flight Center, Greenbelt, MD 20771, September 1970.

5. R. W. Farquhar and A. A. Kamel, "Quasi-Periodic Orbits about the Translunar Libration Point," *Celestial Mechanics*, Vol. 7, 1973, pp. 458–473.

6. D. L. Richardson, "Analytical Construction of Periodic Orbits about the Collinear Points," *Celestial Mechanics*, Vol. 22, 1980, pp. 241–253.

7. D. L. Richardson and N. D. Cary, "A Uniformly Valid Solution for Motion About the Interior Libration Point of the Perturbed Elliptic-Restricted Problem," *Advances in the Astronautical Sciences*, Vol. 33, 1975, AAS 75-021.

8. K. C. Howell and H. J. Pernicka, "Numerical Determination of Lissajous Trajectories in the Restricted Three-Body Problem," *Celestial Mechanics*, Vol. 41, July 1988, pp. 107–124.

9. K. C. Howell and H. J. Pernicka, "Stationkeeping Method of Libration Point Trajectories," *Journal of Guidance, Control, and Dynamics*, Vol. 16, January-February 1993, pp. 151–159.

10. K. C. Howell and B. G. Marchand, "Control Strategies for Formation Flight in the Vicinity of the Libration Points," *Advances in the Astronautical Sciences*, Vol. 113, Part 3, 2003, pp. 197–230, AAS 03-113.

11. S. R. Vadali, H.-W. Bae, and K. T. Alfriend, "Design and Control of Libration Point Satellite Formations," *The 2004 AAS/AIAA Space Flight Mechanics Meeting*, No. AAS 04-161, AAS Publications, Maui, HI, February 2004.

12. D. C. Folta, "Formation Flying Design and Applications in Weak Stability Boundary Regions," *Annals of the New York Academy of Sciences*, Vol. 1017, May 2004, pp. 95–111.

13. W. Ren and R. W. Beard, "Virtual Structure Based Spacecraft Formation Control with Formation Feedback," *AIAA Guidance, Navigation and Control Conference and Exhibit*, No. AIAA 2002-4963, AIAA, Monterey, CA, August 2002.

14. J. Ashenberg, "Satellite Pitch Dynamics in the Elliptic Problem of Three Bodies," *Journal of Guidance, Control, and Dynamics*, Vol. 19, No. 1, January-February 1996, pp. 68–74.

15. H. K. Khalil, *Nonlinear Systems*, Prentice Hall, Upper Saddle River, NJ, 3rd ed., 2002.

16. P. C. Hughes, *Spacecraft Attitude Dynamics*, Wiley, Hoboken, NJ, 1986.

17. B. N. Agarwal, *Design of Geosynchronous Spacecraft*, Prentice Hall, Englewood Cliffs, NJ, 1986.

18. J. L. Junkins and J. D. Turner, *Optimal Spacecraft Rotational Maneuvers*, Elsevier, Amsterdam, The Netherlands, 1986.

19. S. R. Vadali, S. S. Vaddi, and K. T. Alfriend, "An Intelligent Control Concept for Formation Flying Satellites," *International Journal of Robust and Nonlinear Control*, Vol. 12, 2002, pp. 97–115.

20. R. J. Luquette and R. M. Sanner, "Linear State-Space Representation of the Dynamics of Relative Motion, Based on Restricted Three-Body Dynamics," *AIAA Guidance, Navigation, and Control Conference and Exhibit*, No. AIAA-2004-4783, AIAA, Providence, RI, August 2004.